# Fundamental aerodynamics of the soccer ball

**T. Asai,* K. Seo,† O. Kobayashi‡ and R. Sakashita§**

*Comprehensive Human Sciences, Tsukuba University, Tsukuba, Japan
†Faculty of Education, Art & Science, Yamagata University, Yamagata, Japan
‡Department of Aeronautics & Astronautics, Tokai University, Hiratsuka, Japan
§Faculty of Education, Kumamoto University, Kumamoto, Japan

## Abstract

When the boundary layer of a sports ball undergoes the transition from laminar to turbulent flow, a drag crisis occurs whereby the drag coefficient ($C_d$) rapidly decreases. However, the aerodynamic properties and boundary-layer dynamics of a soccer ball are not yet well understood. In this study we showed that the critical Reynolds number ($Re_{crit}$) of soccer balls ranged from $2.2 \times 10^5$ to $3.0 \times 10^5$. Wind-tunnel testing, along with visualisation of the dynamics of the boundary layer and the trailing vortex of a ball in flight, demonstrated that both non-spinning and spinning (curved) balls had low $C_d$ values in the super-critical region. In addition, the $Re_{crit}$ values of the soccer balls were lower than those of smooth spheres, ranging from ~$3.5 \times 10^5$ to $4.0 \times 10^5$, due to the effects of their panels. This indicated that the aerodynamic properties of a soccer ball were intermediate between those of a smooth ball and a golf ball. In a flow visualisation experiment, the separation point retreated and the $C_d$ decreased in a super-critical regime compared with those in a sub-critical regime, suggesting a phenomenon similar to that observed in other sports balls. With some non-spinning and spinning soccer balls, the wake varied over time. In general, the high-frequency component of an eddy dissipated, while the low-frequency component increased as the downstream vortex increased. The causes of the large-scale fluctuations in the vortex observed in the present study were unclear; however, it is possible that a 'knuckle-ball effect' of the non-rotating ball played a role in this phenomenon.

**Keywords:** aerodynamics, football, soccer, visualisation, wind tunnel

## Introduction

Many sports involve throwing, hitting or kicking a ball. However, all sports balls are dynamically affected by air and/or water. Research on golf balls was pioneered by Thompson (1910), and many subsequent studies have focused on golf balls' drag coefficient ($C_d$) values and dimple shapes (Davies, 1949; Bearman & Harvey, 1976; Smits & Ogg, 2004). Tennis balls have been investigated in terms of their basic aerodynamic properties (Stepanek, 1988) and surface-shape effects (Chadwick & Haake, 2000; Haake *et al.*, 2000). For baseballs, the relationship between rotation and lateral forces has been evaluated, as well as the effects of seams on their aerodynamic properties (Watts & Sawyer, 1975; Watts & Ferrer, 1987). Several similar studies have investigated cricket balls (Mehta *et al.*, 1983), volley balls (Wei *et al.*, 1988) and rugby balls (Seo *et al.*, 2004). Many of these reports were reviewed previously by Mehta (1985).

*Correspondence address:*
Takeshi Asai
Comprehensive Human Sciences,
Institute of Health & Sports Science
University of Tsukuba
Tennoudai 1-1-1, Tsukuba 305-8574
Japan
Tel: 029 853 2711
Fax: 029 853 2711
E-mail: asai@taiiku.tsukuba.ac.jp

By contrast, relatively few studies have been carried out on soccer balls (Carré & Asai, 2004; Carré *et al.*, 2004; Carré *et al.*, 2005; Barber *et al.*, 2006). Consequently, the aerodynamic properties of full-size soccer balls have remained unclear. Understanding the flight path of a soccer ball as it curves and drops is essential for the modern game. Hence, there is a need for the aerodynamic properties of soccer balls to be investigated.

In the present study, we compared the aerodynamic coefficients of rotating and non-rotating full-size soccer balls via a wind tunnel experiment. We also investigated the vortex dynamics of soccer balls in flight, using a titanium tetrachloride visualisation method, in order to clarify their aerodynamic properties.

## Methods

### Wind tunnel tests

This experiment used a low-speed circulating wind tunnel with a six-component balance (maximum wind velocity = 40 m $s^{-1}$; measuring section = 1.5 × 1 m; turbulence level = 1%) at the Department of Aeronautics & Astronautics, Tokai University, Japan. Tests were performed on a hand-stitched soccer ball with panels (Size 5 Adidas Fevernova), and two thermally bonded soccer balls with panels (Size 5 Adidas Roteiro and Size 5 Adidas Teamgeist), all of which were officially approved for use in international games. Each ball was supported at the rear, with the sting fitted to the six-component wind tunnel balance (Fig. 1). Each ball was fixed to the sting with an adhesive, so that it could not rotate.

For the measurements of a spinning ball, a full-size model of an internationally approved soccer ball (Teamgeist) was moulded with fibre-reinforced plastic (FRP) (Fig. 2), and supported at the sides with piano wire (diameter = 2 mm). The ball was spun with an air compressor, and the number of revolutions was calculated with a tachometer.

The following parameters were calculated from experimental data collected over a range of conditions: the wind velocity ($U$); the force acting in the opposite direction to the wind, known as drag ($D$); the force acting perpendicular to the wind direction, known as lift ($L$); and the force acting sideways based on a frontal view ($S$). The aerodynamic forces detected in the experiment were converted to the drag coefficient ($C_d$), the lift coefficient ($C_l$) and the lateral-force coefficient ($C_s$), as shown in eqns. 1–3.

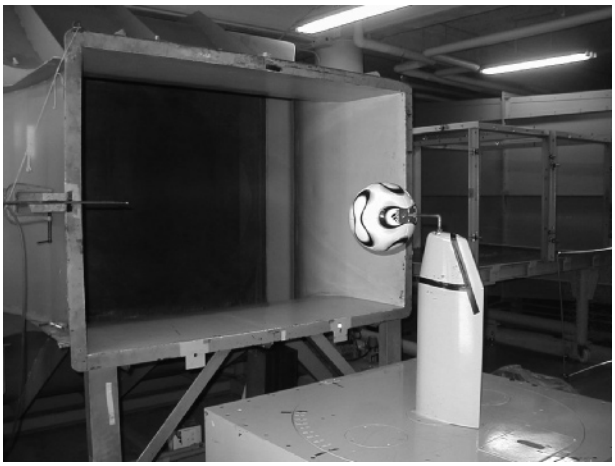

**Figure 1** Wind tunnel experimental set-up for a non-rotating ball. The ball was supported at the back, with the tip mounted on a six-component wind tunnel balance.

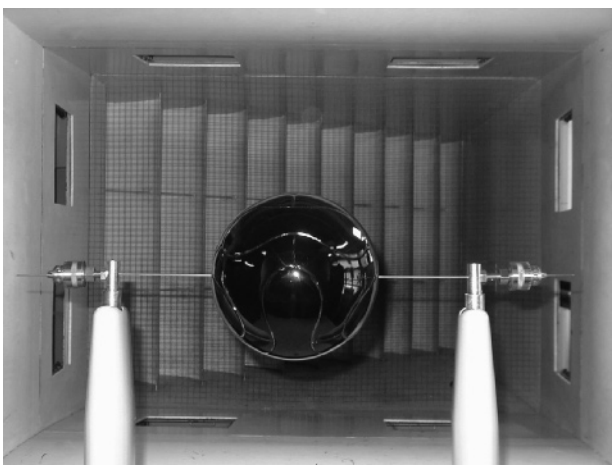

**Figure 2** Wind tunnel experimental set-up for a rotating ball. An FRP ball model was supported via bearings with piano wire (diameter = 2 mm) stretched horizontally from left to right.

$$C_d = \frac{D}{\frac{1}{2}\rho U^2 A} \quad (1)$$

$$C_l = \frac{L}{\frac{1}{2}\rho U^2 A} \quad (2)$$

$$C_s = \frac{S}{\frac{1}{2}\rho U^2 A} \quad (3)$$

Here, $\rho$ is the density of air (1.2 kg m$^{-3}$), $U$ is the flow velocity (m s$^{-1}$) and $A$ is the projected area of the soccer ball ($r^2$, where $r$ is the radius). The wind velocity used in the tunnel experiment was within the range of 7–35 m s$^{-1}$ for non-rotating balls.

The balls were rotated using an air compressor during the wind tunnel experiment. An air gun connected to an air compressor was fired at the side of each ball, and the number of rotations was measured using a laser tachometer. The angular velocity became unstable during low-speed rotation. Most curve kicks produce a ball velocity of at least 20 m s$^{-1}$ (Asai *et al.*, 2002). We therefore studied the aerodynamic properties of a rotating ball with a flow velocity in the range of 22–30 m s$^{-1}$ and a rotational speed of 2–10 revolutions per second (rev s$^{-1}$). $S_p$ was defined as the ratio of the peripheral velocity to the velocity through the air, as shown in eqn. 4.

$$S_p = \frac{R}{U} \tag{4}$$

Here, $\omega$ is the angular velocity of the ball in radians per second (rad s$^{-1}$), and $R$ is the radius of the ball (0.11 m).

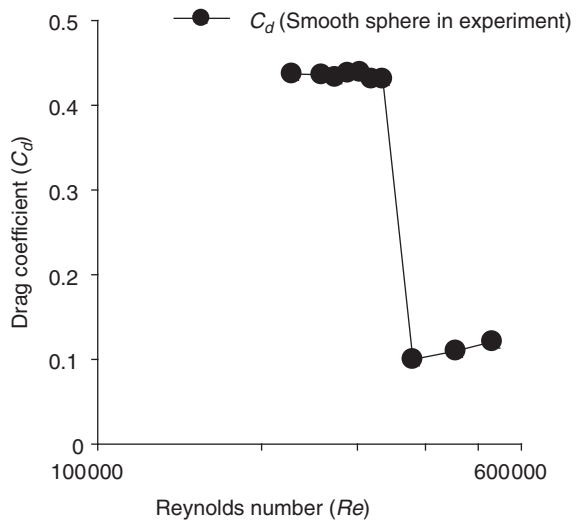


**Figure 3** Aerodynamic characteristics of a smooth sphere used to verify the wind tunnel set-up. The sub-critical and super-critical $C_d$ values of a smooth sphere were expected to be ~0.5 and ~0.1, respectively. The $Re_{crit}$ at which the boundary layer shifts from laminar to turbulent is reportedly ~3.5 × 10$^5$ (Achenbach, 1972). Using this wind tunnel set-up, the sub-critical and super-critical $C_d$ values of a smooth sphere were ~0.45 and ~0.1, respectively.

We also investigated the aerodynamic characteristics of a smooth sphere, in order to verify the wind tunnel set-up used in this study. The sub-critical and super-critical $C_d$ values of a smooth sphere are reported to be ~0.5 and ~0.1, respectively. Moreover, the critical Reynolds number ($Re_{crit}$) value at which the boundary layer shifts from laminar to turbulent is reportedly ~3.5 × 10$^5$ (Achenbach, 1972). Using the wind tunnel set-up described above, the sub-critical and super-critical $C_d$ values of a smooth sphere were found to be ~0.45 and ~0.1, respectively (Fig. 3). The $C_d$ values of the sub-critical regime in this study were slightly smaller than the values reported by Achenbach (1972). The $C_d$ values of the super-critical regime in this study were similar to those reported by Achenbach (1972). The $Re_{crit}$ value of the smooth sphere produced using this experimental set-up was ~3.5 × 10$^5$, which was similar to the value reported by Achenbach (1972). Therefore, we considered the experimental data generated using the wind tunnel set-up in the current study to be suitable for further investigations.

## Flow visualisation

A visualisation experiment using titanium tetrachloride (Asai *et al.*, 2006) was conducted in order to visualise the flow around a soccer ball during flight. The soccer ball was placed directly in front of a soccer goal, at a distance of 15 m, and a subject performed a straight kick with little rotation as well as a side-spinning curve kick aimed at the goal. Both placement kicks were delivered at the same velocity, to mimic the conditions in a soccer game (Asai *et al.*, 1998). A high-speed video tape recorder (VTR) camera (Photron Ultima; Photron Limited) was set up at a midpoint between the spot where the ball was placed and the soccer goal, and photographs were taken at 4500 frames s$^{-1}$.

The experimental procedure was as follows. Each soccer ball was brush-painted with titanium tetrachloride, placed on a designated spot and then kicked towards the goal. As the ball moved towards the goal, the air flow around it was revealed by white smoke produced by the titanium tetrachloride. Photographs were taken using a high-speed video camera. Finally, the ball was collected and cleaned.

## Results and discussion

### Non-rotating balls

In the visualisation experiment, the soccer ball was not completely non-rotating. Therefore, both non-rotating and slowly-rotating (0.5 rev $s^{-1}$) soccer balls were categorised together, and treated as non-rotating systems in the analysis.

In the wind tunnel experiment, changes in drag in relation to wind speed were observed for an officially approved 2004 Roteiro soccer ball. The drag increased from 0.5 to 3.8 N as the wind speed rose from 7 to 35 m $s^{-1}$. However, these changes were not uniform. When the wind speed was ~12–15 m $s^{-1}$, a drag crisis was observed, whereby the drag decreased (Asai *et al.*, 1998). The drag crisis occurred through 'transition' from a laminar boundary layer to a turbulent boundary layer on a sphere (Achenbach, 1972). A similar trend has been observed in other sports balls.

The $Re_{crit}$ values were ~$2.2 \times 10^5$ for the officially approved 2002 Fevernova soccer ball and the Roteiro soccer ball, and ~$3.1 \times 10^5$ for the officially approved 2006 Plus Teamgeist soccer ball (Fig. 4). In general, the sub-critical and super-critical $C_d$ values of a smooth sphere are expected to be ~0.5 and 0.1, respectively. Moreover, the $Re_{crit}$ value at which the boundary layer shifts from laminar to turbulent is reportedly ~$3.5 \times 10^5$ (Achenbach, 1972). By contrast, the boundary layer is considered to shift at a lower value for a soccer ball.

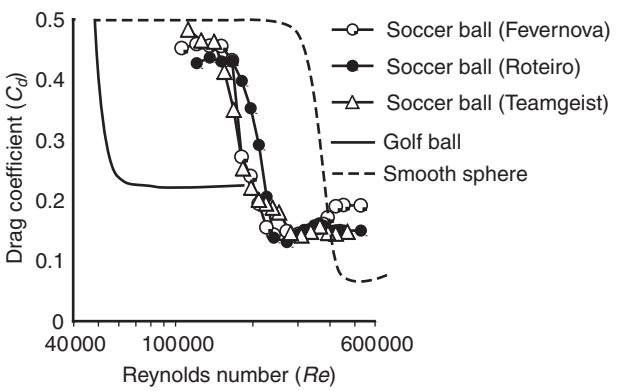


**Figure 4** Relationship between the *Re* and $C_d$ for non-rotating soccer balls. The Roteiro and Teamgeist balls had slightly lower $C_d$ values than the Fevernova ball in the super-critical range. (Adapted from Bearman & Harvey, 1976 and Achenbach, 1972.)

In a previous wind tunnel experiment using a ⅓ scale model soccer ball (Carré & Asai, 2004), the $Re_{crit}$ value of a non-rotating ball was found to be ~$1.3 \times 10^5$, which was lower than that calculated in the present study. This discrepancy could have been caused by the seams, which were expected to affect the model soccer ball to a comparatively greater extent. The surface panels on the Roteiro and Teamgeist soccer balls used in the present study were not hand-stitched but thermally bonded, and the small surface indentations might have also affected the results. Furthermore, the Fevernova and Roteiro balls had 32 panels, while the Teamgeist ball had 14 panels, so the drag properties of the latter were expected to more closely resemble those of a smooth sphere. The $C_d$ values of the Roteiro and Teamgeist balls in the super-critical range were slightly lower than that of the Fevernova ball, and the surface processing and stitching might have affected this parameter (Achenbach, 1974). The $C_d$ values appeared to depend upon the roughness of the ball surface to a great extent, and the large seams might have caused additional boundary-layer separation.

These findings suggest that the drag properties of a soccer ball are intermediate between those of a smooth sphere and a golf ball. When a soccer player takes a powerful shot or a free kick, the initial speed is generally in the range of ~25–35 m $s^{-1}$ (Asai *et al.*, 2002); the ball is thus predicted to reach the goal before it is affected by the $Re_{crit}$ region. As a soccer ball has a lower $Re_{crit}$ value than a smooth sphere, and there is a broader range of speeds in the super-critical region, the panelling on a ball is thought to lower the aerodynamic drag by speeding up the timing of the drag crisis.

The images from the visualisation experiment were examined based on the angle of the boundary layer separation point from the front stagnation point (that is, the front of ball). We initially compared the flow around the ball during a non-rotating low-velocity kick (5 m $s^{-1}$) and a high-velocity kick (29 m $s^{-1}$) (Figs. 5–6). During the low-velocity kick, the boundary layer separation point was ~90° from the front stagnation point and the vortex region was comparatively large. By contrast, during the high-velocity kick, the separation point receded to ~120° from the front stagnation point and the vortex region shrank.

The $Re_{crit}$ value during the transition to turbulence of a non-spinning smooth ball is reportedly ~$3.5 \times 10^5$; separation below the $Re_{crit}$ occurs at ~75° from the front stagnation point, while that above the $Re_{crit}$ occurs at ~135° from the front stagnation point (Taneda, 1978). For the soccer ball, the difference in values before and after transition was relatively small, although it reached ~30° and was accompanied by a difference in the vortex region. The angle of the boundary layer separation point from the front stagnation point is often used as an indicator of the size of the vortex region; however, when the vortex deviates due to factors such as rotation, the angle from the front stagnation point cannot always be measured accurately.

An examination of the relationship between the non-rotating soccer ball vortex angle (2 – ; both side angles from the front stagnation point) and the *Re* in the present study revealed that the former was ~180° in the sub-critical region and ~120° in the super-critical region. From this finding, we inferred that the $C_d$ also decreased in the super-critical region.

The flight trajectory resulting from a non-rotating kick ($U$ = 25 m s$^{-1}$) was filmed at a wider angle of view, revealing ~50 vortex s$^{-1}$. The results of repeated kicks showed a similar trend (Fig. 7). Large-scale undulation of the vortex trail was observed in each experiment. In

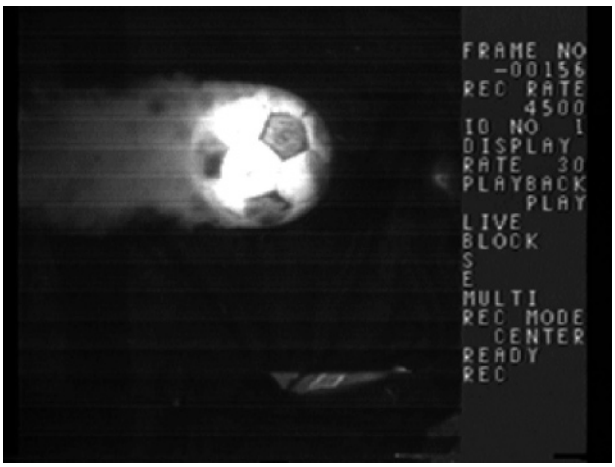


**Figure 5** Visualisation of the flow around the ball after a low-velocity kick (5 m s$^{-1}$). The boundary layer separation point was ~90° from the front stagnation point. The ball was thought to be in flight in the sub-critical range. The flow was from right to left.

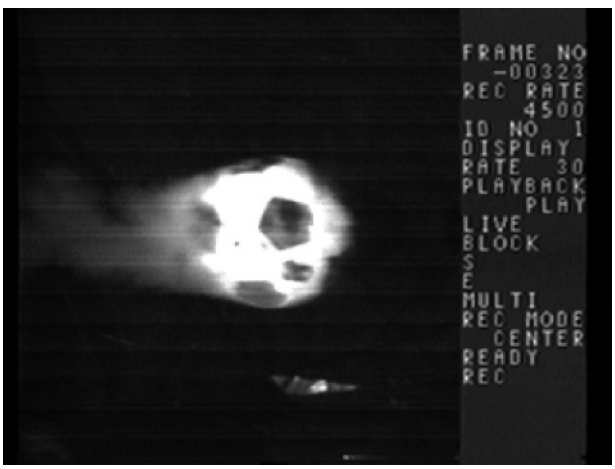


**Figure 6** Visualisation of the flow around the ball after a high-velocity kick (29 m s$^{-1}$). The boundary layer separation point receded to ~120° from the front stagnation point. The ball was thought to be in flight in the super-critical range. The flow was from right to left.

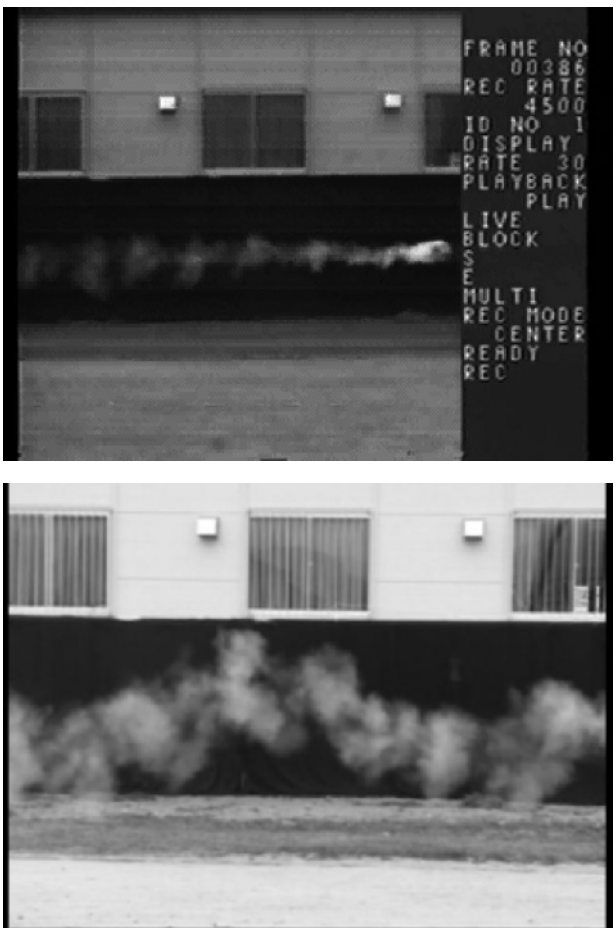


**Figure 7** Vortex pathway for a non-rotating ball viewed from a wide angle.
**(a)** Large-scale fluctuations were observed over time.
**(b)** The flow was from right to left.

general, the high-frequency component of an eddy dissipates while the low-frequency component increases as the downstream vortex increases. The causes of the large-scale fluctuation in the vortex observed in the present study were unclear; however, it is possible that a 'knuckle-ball effect' of the non-rotating ball played a part. This phenomenon causes irregularity and erratic movements of a soccer ball during flight. The effects of the power spectrum and vortex Strouhal number on the aerodynamic properties of non-rotating soccer balls should be investigated in future studies.

## Rotating ball

The $C_d$ of a rotating ball was found to increase linearly as the spin parameter ($S_p$) increased (Fig. 8). In fact, our data strongly suggested that the $C_d$ during ball rotation was highly dependent upon the $S_p$. A similar trend was observed in wind tunnel experiments on golf balls (Bearman & Harvey, 1976). This indicates that as the number of rotations increases, the $S_p$ and $C_d$ increase. Thus, the more the ball is rotated by a curve kick at a constant speed, the more it will be affected by wind resistance and become airborne. Assuming that the angular velocity of the ball ($\omega$) is constant, $S_p$ and $C_d$ will decrease as $Re$ increases. The revolution ratio of the ball measured in the present study did not exceed 10 rev s$^{-1}$, based on actual curve kicks; however, in cases with a higher revolution ratio, it is possible that different properties might be shown.

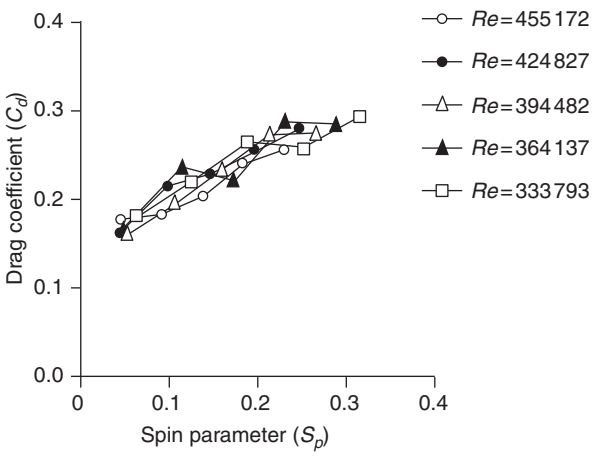


**Figure 8** Relationship between $S_p$ and $C_d$ for rotating balls. The $C_d$ tended to increase as the $S_p$ increased. The $C_d$ was largely independent of speed, but appeared to be highly dependent upon the $S_p$.

The $C_d$ is largely independent of the $Re$ and, therefore, the velocity. The relationship between the number of ball revolutions and the $C_d$ is thus unrelated to the ball speed. The results of the present study demonstrated that when a high-speed curve kick was made from an actual free kick (Asai *et al.*, 2002), the ball had a comparatively small $C_d$ (0.3).

The $C_s$, which corresponds to the Magnus force coefficient, increased in a curved manner as the $S_p$ increased (Fig. 9). When the $S_p$ was 0.1, the $C_s$ decreased to 0.1. However, when the above mentioned effect was excluded, a linear relationship was observed. Further detailed measurements will thus be needed to determine whether the course is curved or linear. However, in either case, the $C_s$ tended to increase as the $S_p$ increased (Smits & Ogg, 2004). When the number of revolutions increased at a constant ball speed, the $C_s$ also increased. This was expected on the basis of the Magnus force (Magnus, 1852; Briggs, 1959). When the number of revolutions was constant, the $C_s$ decreased as the speed of the ball increased. Therefore, the more the ball rotated, the greater the $C_s$. This meant that, although the ball had a curve, the rate of curvature decreased as the speed increased. These data are valuable for calculating the ball trajectory (Carré *et al.*, 2002). Our findings also suggest that when a soccer ball is in flight at 26 m s$^{-1}$ and 8 rev s$^{-1}$, it is deflected at ~4 m s$^{-1}$ due to the Magnus effect.

In the visualisation experiment, side-view images of a spinning ball at 26 m s$^{-1}$ and 8 rev s$^{-1}$ ($S_p$ = 0.21)

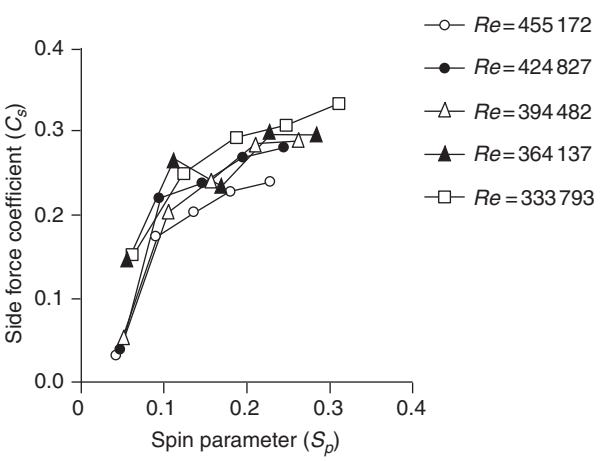


**Figure 9** Relationship between $S_p$ and $C_s$ for a rotating ball. The $C_d$ tended to increase in a curved manner as the $S_p$ increased.

showed that the separation point was positioned ~120° from the stagnation point, and that the boundary layer between the top and bottom surfaces of the ball was turbulent (Fig. 10). The flow was from right to left. In this instance, the vortex angle was 120°, which was similar to that of a non-rotating ball. The dynamics of the ball vortex revealed a vortex ring with comparatively little loss of form. However, as eddies are sometimes seen with a loss of form, the mechanism and detailed dynamics of this phenomenon need to be studied further.

The top-view images of a rotating ball at 27 m $s^{-1}$ and 7 rev $s^{-1}$ ($S_p$ = 0.18) demonstrated that the vortex deviated and flowed like a 'downwash', due to the effects of the relative difference in fluid speed caused by the rotation (Fig. 11). The flow was from right to left. The force acting in a lateral direction due to a counteraction to this vortex was a major reason for the curvature, which was also related to the $C_s$. However, the separation point was not symmetrical on the left and right in relation to the direction of travel (top and bottom symmetry in Fig. 10), the vortex angle reached ~128°, which differed slightly from the ~120° vortex angle during non-rotation. This finding suggests that, during rotation, the boundary layer becomes turbulent, and the ball flies with a comparatively small vortex region. The $S_p$ in this case was ~0.18, and both the $C_d$ and $C_s$ were estimated to be ~0.25. These results show that for rotating balls, the boundary layer from the position of the separation point and the vortex region is turbulent when the flow velocity is in the range of 22–30 m $s^{-1}$. The $C_d$ of the rotating ball in the wind tunnel experiment was also relatively low, which supported the visualisation data. The flow velocity measured in the present study had a comparatively small range (22–30 m $s^{-1}$) in relation to the actual ball flight velocity. Future studies should thus repeat these measurements over a broader range of velocities and revolutions per second.

The current wind tunnel experiment analysed a constant state – that is, the mean characteristics over a given length of time. However, actual soccer ball-related flow-dynamic phenomena are often non-stationary for periods of ~1 s (Asai *et al.*, 2002). We therefore recommend that further research should be carried out in the non-stationary region.


**Figure 10** Series of side-view lateral images of a rotating ball in flight at 26 m $s^{-1}$ and 8 rev $s^{-1}$ ($S_p$ = 0.21). The time interval for each image was ~0.0067 s. The separation point was ~120° from the front stagnation point, and the vortex angle also reached ~120°. The flow was from right to left.


**Figure 11** Series of top-view parietal images of a rotating ball in flight at 27 m $s^{-1}$ and 7 rev $s^{-1}$ ($S_p$ = 0.18). The time interval for each image was ~0.0067 s. The vortex deviated, and the vortex angle reached ~128°. The flow was from right to left.

## Conclusions

The present study used a wind tunnel experiment to determine the aerodynamic coefficients of rotating and non-rotating soccer balls. In addition, a visualisation experiment using titanium tetrachloride investigated the dynamics of the vortex of a soccer ball in flight, and attempted to elucidate its aerodynamic properties. According to the wind tunnel experiment, the $C_d$ of a non-rotating soccer ball was ~0.43 in the sub-critical region and ~0.15 in the super-critical region, suggesting that the $Re_{crit}$ value was in the range of ~$2.2–3.0 \times 10^5$. The $C_d$ and $C_s$ of a rotating ball both increased as the $S_p$ increased. The visualisation experiment revealed that during a low-speed kick (5 m $s^{-1}$), the boundary-layer separation point of a non-rotating ball was ~90° from the front stagnation point, whereas it receded to ~120° during a high-speed kick (29 m $s^{-1}$). It was assumed that, for a rotating ball, the boundary layer would be turbulent because the separation point receded and the vortex angle shrank. This suggested that the $C_d$ was also comparatively low. Thus, the results of the wind tunnel experiment were supported by the visualisation data. Broader-angle imaging of the flight trajectory of a non-rotating ball revealed a large-scale undulation of the vortex trail, which might influence the knuckle-ball effect in soccer.

## References

Achenbach, E. (1972) Experiments on the flow past spheres at very high Reynolds numbers. *Journal of Fluid Mechanics*, **54**, 565–575.

Achenbach, E. (1974) The effects of surface roughness and tunnel blockage on the flow past spheres. *Journal of Fluid Mechanics*, **56**, 113–125.

Asai, T., Akatsuka, T. & Haake, S.J. (1998) The physics of football. *Physics World*, **11**, 25–27.

Asai, T., Carré, M.J., Akatsuka, T. & Haake, S.J. (2002) The curve kick of a football, I: impact with the ball. *Sports Engineering*, **5**(4), 183–192.

Asai, T., Seo, K., Kobayashi, O. & Sakashita, R. (2006) Flow visualization on a real flight non-spinning and spinning soccer ball, in E.F. Moritz & S.J. Haake (eds) *The Engineering of Sport 6*, Vol. 1, pp. 327–332. International Sports Engineering Association, Sheffield.

Barber, S., Haake, S.J. & Carré, M.J. (2006) Using CFD to understand the effects of seam geometry on soccer ball aerodynamics, in *The Engineering of Sport 6*, Vol. 2,

pp. 127–132. International Sports Engineering Association, Sheffield.
Bearman, P.W. & Harvey, J.K. (1976) Golf ball aerodynamics. *Aeronautical Quarterly*, **27**, 112–122.
Briggs, L.J. (1959) Effect of spin and speed on the lateral deflection (curve) of a baseball; and the Magnus effect for smooth spheres. *American Journal of Physics*, **27**, 589–596.
Carré, M.J. & Asai, T. (2004) Biomechanics and aerodynamics in soccer, in G.K. Hung & J.M. Pallis (eds) *Biomedical Engineering Principles in Sports*, pp. 333–364. Kluwer Academic Plenum Publishers, New York.
Carré, M.J., Asai, T., Akatsuka, T. & Haake, S.J. (2002) The curve kick of a football, II: flight through the air. *Sports Engineering*, **5**(4), 193–200.
Carré, M.J., Goodwill, S.R., Haake, S.J., Hanna, R.K. & Wilms, J. (2004) Understanding the aerodynamics of a spinning soccer ball, in M. Hubbard, R.D. Mehta & J.M. Pallis (eds) *The Engineering of Sport 5*, Vol. 1, pp. 70–76. International Sports Engineering Association, Sheffield.
Carré, M.J., Goodwill, S.R. & Haake, S.J. (2005) Understanding the effect of seams on the aerodynamics of an association football. *Proceedings of the Institution of Mechanical Engineers, Part C: Journal of Mechanical Engineering Science*, **219**, 657–666.
Chadwick, S.G. & Haake, S.J. (2000) The drag coefficient of tennis balls, in A. Subic & S.J. Haake (eds) *The Engineering of Sport*, pp. 169–176. Blackwell Science, Oxford.
Davies, J.M. (1949) The aerodynamics of golf balls. *Journal of Applied Physics*, **20**, 821–828.
Haake, S.J., Chadwick, S.G., Dignall, R.J., Goodwill, S.R. & Rose, P. (2000) Engineering tennis – slowing the game down. *Sports Engineering*, **3**, 131–143.
Magnus, G. (1852) On the derivation of projectiles; and on a remarkable phenomenon of rotating bodies, in J. Tyndall & W. Francis (eds) *Memoirs of the Royal Academy*, Berlin, Germany. English translation in *Scientific Memoirs*, p. 210. London (1853).
Mehta, R. (1985) Aerodynamics of sports balls. *Annual Review of Fluid Mechanics*, **17**, 151–189.
Mehta, R.D., Bentley, K., Proudlove, M. & Varty, P. (1983) Factors affecting cricket ball swing. *Nature*, **303**, 787–788.
Seo, K., Kobayashi, O. & Murakami, M. (2004) Regular and irregular motion of a rugby football during flight, in M. Hubbard, R.D. Mehta & J.M. Pallis (eds) *The Engineering of Sport 5*, Vol. 1, pp. 567–573. International Sports Engineering Association, Sheffield.
Smits, A.J. & Ogg, S. (2004) Aerodynamics of golf ball, in G.K. Hung & J.M. Pallis (eds) *Biomedical Engineering Principles in Sports*, pp. 333–364. Kluwer Academic Plenum Publishers, New York.
Stepanek, A. (1988) The aerodynamics of tennis balls – the topspin lob. *American Journal of Physics*, **56**, 138–142.
Taneda, S. (1978) Visual observations of the flow past a sphere at Reynolds numbers between $10^4$ and $10^6$. *Journal of Fluid Mechanics*, **85**, 187.
Thompson, J.J. (1910) The dynamics of a golf ball. *Nature*, **85**, 2151–2157.
Watts, R.G. & Ferrer, R. (1987) The lateral force on a spinning sphere: aerodynamics of a curveball. *American Journal of Physics*, **55**, 40–44.
Watts, R.G. & Sawyer, E. (1975) Aerodynamics of a knuckleball. *American Journal of Physics*, **43,** 960–963.
Wei, Q., Lin, R. & Liu, Z. (1988) Vortex-induced dynamics loads on a non-spinning volleyball. *Fluid Dynamics Research*, **3**, 231–237.